

基于移动 Kriging 插值无网格法的多层纳米板 振动特性研究

侯东昌¹, 张吉成², 王立峰²

(1. 中原工学院建筑工程学院, 河南 郑州 450007;
2. 南京航空航天大学航空航天结构力学及控制全国重点实验室, 江苏 南京 210016)

摘要: 采用基于移动 Kriging 插值的无网格法研究了多层纳米板的动力学行为。建立了考虑层内拉伸、层间剪切和单层弯曲的多层二硫化钼动力学模型。通过与分子动力学模拟的结果比较表明, 建立的多层纳米板模型能够很好地预测多层二硫化钼的振动行为。多层二维结构层间剪切和滑移导致其违背了经典板理论的预测, 主要归因于二维结构之间的层间剪切影响了其整体动力学行为。分析了层数和尺寸对振动频率的影响, 研究了层内拉伸刚度、层间剪切模量和单层弯曲刚度对振动频率的影响。

关键词: 多层纳米板; 层间剪切; 移动 Kriging 插值; 无网格法; 多层二硫化钼

中图分类号: TB383; O326 **文献标志码:** A **文章编号:** 1004-4523(2025)03-0623-08

DOI: 10.16385/j.cnki.issn.1004-4523.2025.03.019

Vibration characteristics of multilayer nanoplates via meshfree moving Kriging interpolation method

HOU Dongchang¹, ZHANG Jicheng², WANG Lifeng²

(1. School of Civil Engineering and Architecture, Zhongyuan University of Technology, Zhengzhou 450007, China;
2. State Key Laboratory of Mechanics and Control for Aerospace Structures, Nanjing University of Aeronautics and Astronautics,
Nanjing 210016 China)

Abstract: A meshless method based on moving Kriging interpolation is used to study the dynamic behavior of multilayer nanoplates. A dynamical model of multilayer molybdenum disulfide (MoS_2) is established considering intra-layer stretching, interlayer shear and single layer bending. Compared with the results of molecular dynamics simulation, it is shown that the present model can predict the vibration behavior of multilayer MoS_2 . The interlayer shear and slip of multilayer two-dimensional structures violate the prediction of classical plate theory, mainly due to the effect of interlayer shear and slip on the overall dynamic behavior of two-dimensional structures. The influence of different layer number and size on the frequency is investigated, and the influence of the three factors on the frequency is studied by changing the intralayer tensile stiffness, interlayer shear modulus and single layer bending stiffness.

Keywords: multilayer nanoplate; interlayer shear; moving Kriging interpolation; meshfree method; multilayer MoS_2

多层二维结构的层间相互作用可以显著影响层内键合, 能带结构和晶格振动, 表现出与层相关的电子、光学、热、机械和振动特性^[1]。多层二维结构的拉伸荷载通过层间剪切传递, 因此, 充分掌握二维结构层间剪切规律, 对于需精准操纵和控制的二维结构柔性电子器件^[2]和应变半导体^[3]等技术的应用至关重要。多层二维结构的弯曲刚度与经典板理论的预测结果不符, 主要归因于层间剪切和滑移, 二维结

构之间的层间剪切和滑移与层内拉伸和弯曲变形存在竞争, 并影响整体力学响应。早期的研究通常将多层二维结构等效为单层板^[4-6], 显然上述效应在经典板理论中是不存在的, 经典板理论的基本假设不包含层间滑动^[7]。已有基于摩擦显微镜^[8-9]和原子力显微镜^[10-11]的实验研究揭示了二维结构层间剪切行为。然而这些研究对多层二维结构的层间变形和破坏机制的解释有限, 且并未给出层间剪切的定量表

收稿日期: 2024-01-26; 修订日期: 2024-04-22

基金项目: 国家杰出青年科学基金资助项目(11925205); 国家自然科学基金资助项目(51921003, U2341230)

征。即使是已获得广泛关注的石墨烯,对其层间剪切刚度的测量研究也是相对匮乏的。YAMASHITA 等^[12]对高度各向异性的天然石墨进行静态实验,测得层间剪切刚度 τ 在 0.25~0.75 MPa 之间。BLACKSLEE 等^[13]测量得到压缩退火热解石墨层间的剪切刚度 τ 为 0.9~2.5 MPa。LIU 等^[14]通过对石墨台面上微米石墨薄片的自缩回运动^[15]和微米超润滑现象^[16]的观察得到 τ 大约为 0.14 GPa。使用传统的静态力学实验测量层间抗剪强度的主要挑战是无法获得足够大的单晶石墨^[17]。分子动力学模拟的准确性取决于势函数的选取^[18-19]。LEBEDEVA 等^[20]指出,使用 Lennard-Jones(L-J)势计算多层石墨烯层间相互作用能时,其大小被低估了一个数量级。SHEN 等^[18]对双层石墨烯进行了滑动模拟,并计算了层间剪切模量,通过修改 AI-REBO 电位中的 L-J 参数以拟合实验结果。基于以上分析不难发现建立合理的考虑层间剪切的连续介质模型对研究多层二维结构力学行为至关重要^[21]。LIU 等^[22]提出了一个忽略层内拉伸而考虑层间剪切的多层梁模型,该模型将层间剪切角简化为挠度的一阶导数。HUANG 等^[23]建立了考虑层内拉伸、层间剪切和单层弯曲的多层板模型,构建的通用分析框架可直观地展示层内拉伸、层间剪切和单层弯曲三者主导变形的转变和竞争机制。LIU 等^[24]采用分子动力学模拟并结合建立的考虑层间剪切的非线性夹层板模型研究了双层二硫化钼的非线性振动行为。ZHANG 等^[25]研究了层间剪切对双层二维结构振动的影响。通过扭转双层二硫化钼的角度,使结构的固有频率出现了异乎寻常的结果,由此提出了层间负剪切的概念来解释这一现象。随后 ZHANG 等^[26]采用分子动力学模拟研究了不同堆垛的双层黑磷的振动行为,并建立了正交各向异性层合板模型。通过层合板模型得到了层间剪切方向和高阶模态形状与对应频率之间的关系。LIU 等^[27]通过分子动力学和考虑非均匀层间剪切的夹层板模型研究了扭转双层二硫化钼的动力学行为。结果表明,在很小的扭转角下,莫尔条纹会导致层间范德华能在几十纳米尺度上的对称性被破坏,并导致扭曲的双层二硫化钼的动态行为表现出很强的位置依赖性。

从以上分析不难看出,建立可描述层间剪切的多层纳米板模型对研究多层二维纳米结构的力学行为至关重要。同时此类模型的求解通常较为复杂,很难获得其解析解,因此往往需要借助数值方法求解。无网格法构造高阶形函数时所展现出来的优势深受学者们的青睐^[28-29]。文献[30-31]采用基于移动最小二乘近似的无网格法,结合高阶 Cauchy-Born

准则研究了碳纳米管的屈曲。YAN 等^[32-33]采用移动 Kriging 插值研究了碳纳米管的屈曲。随后 YAN 等^[34]采用移动 Kriging 插值研究了圆形石墨烯扭转中波纹幅度、波数和起皱角度的可控性。ROQUE 等^[35]采用径向点插值的无网格法获得了基于修正的偶应力理论的各向同性纳米板弯曲的数值解。THAI 等^[36]采用移动 Kriging 插值研究了基于应变梯度理论的磁电耦合功能梯度纳米板的自由振动。随后 THAI 等^[37]又将非局部应变梯度理论,高阶剪切理论以及移动 Kriging 插值的无网格法相结合,建立了一种非局部应变梯度无网格法用于研究夹层纳米板的弯曲和自由振动。WANG 等^[38-39]基于移动最小二乘发展了一种高阶一致性的节点积分方案求解一系列应变梯度薄梁/板问题,数值结果表明,一致性积分在收敛性、精度以及计算效率方面都优于标准高斯积分。ALSHENAWY 等^[40]采用移动 Kriging 插值研究了在轴向机械荷载、外电驱动和温度共同作用下,功能梯度压电纳米圆柱壳的屈曲模态转变现象。YANG 等^[41]采用移动 Kriging 插值研究了基于偶应力理论的复合材料纳米圆柱壳的后屈曲行为。LIU 等^[42]采用移动 Kriging 插值的无网格法研究了随机增强纳米复合材料制成的微圆柱壳在轴向和侧向压缩组合作用下的非线性屈曲和后屈曲。

本文采用基于移动 Kriging 插值的无网格法研究多层纳米板的动力学行为。首先建立考虑层内拉伸、层间剪切和单层弯曲的多层二硫化钼动力学模型。随后将所建立的模型与分子动力学,等效单层 Kirchhoff 板模型和 Mindlin 板模型的结果进行比较。分析不同层数和尺寸对振动频率的影响,并通过改变层内拉伸刚度、层间剪切模量和单层弯曲刚度的大小,研究三者对振动频率的影响。

1 考虑层间剪切的多层板模型

多层二维纳米结构之间既没有超润滑,也没有完全贴合,每一层厚度方向的尺度仅一个或几个原子,而长、宽方向的尺度远大于厚度方向,因此将其等效为多层薄板堆叠模型,如图 1 所示。当其发生横向振动时会伴随着层间剪切和滑移,因此传统板模型中平截面假定不再适用。多层板模型厚度方向依旧远小于长、宽方向的尺寸,即假设每层板具有相同的挠度,因此该模型中每层板 z 方向的变形可等效为一个 w ,而每一层板的面内位移包括 u 和 v 两部分。

考虑层内拉伸、层间剪切和弯曲变形的多层二维结构自由振动的总势能包括以下三部分:

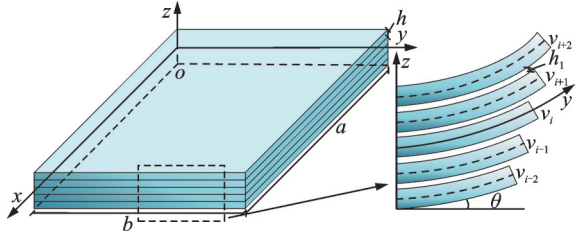


图 1 多层板模型示意图

Fig. 1 Schematic diagram of multilayer plate model

$$U = U_T + U_S + U_B \quad (1)$$

式中, U_T 为层内拉伸应变能; U_S 为层间剪切能; U_B 为弯曲能。

二维平面内层内拉伸应变能可表示为:

$$U_T = \frac{1}{2} \iint \sum_{i=1}^N \epsilon_i^T D_T \epsilon_i dx dy \quad (2)$$

式中, i 表示第 i 层, $\epsilon_i = \begin{bmatrix} \frac{\partial u_i}{\partial x} \\ \frac{\partial v_i}{\partial y} \end{bmatrix}$; $D_T = \begin{bmatrix} Eh & \\ & Eh \end{bmatrix}$, h 为

单层板厚度, E 为弹性模量。

由于考虑层内拉伸, 层与层之间的剪切角应包含两部分, 分别为相邻层间滑移部分以及层内的弯曲产生的剪切角, 因此层间剪切能可表示为:

$$\begin{aligned} U_S = & \frac{1}{2} G_x h_1 \iint \sum_{i=2}^N \left(\frac{1}{h_1} \Delta u_i + \frac{dw}{dx} \right)^2 dx dy + \\ & \frac{1}{2} G_y h_1 \iint \sum_{i=2}^N \left(\frac{1}{h_1} \Delta v_i + \frac{dw}{dy} \right)^2 dx dy = \\ & \frac{1}{2} G_x h_1 \iint \sum_{i=2}^N \left[\frac{\Delta u_i^2}{h_1^2} + 2 \frac{\Delta u_i}{h_1} \frac{dw}{dx} + \left(\frac{dw}{dx} \right)^2 \right] dx dy + \\ & \frac{1}{2} G_y h_1 \iint \sum_{i=2}^N \left[\frac{\Delta v_i^2}{h_1^2} + 2 \frac{\Delta v_i}{h_1} \frac{dw}{dy} + \left(\frac{dw}{dy} \right)^2 \right] dx dy \end{aligned} \quad (3)$$

式中, G_x 和 G_y 分别为沿 x 轴和 y 轴方向的剪切模量; N 为总层数; h_1 为层间剪切距离。

多层板的弯曲能为:

$$\begin{aligned} U_B = & \frac{1}{2} D \iint \sum_{i=1}^N \left\{ (\nabla^2 w)^2 - 2(1-\mu) \left[\frac{\partial^2 w}{\partial x^2} \frac{\partial^2 w}{\partial y^2} - \right. \right. \\ & \left. \left. \left(\frac{\partial^2 w}{\partial x \partial y} \right)^2 \right] \right\} dx dy \end{aligned} \quad (4)$$

式中, $D = Eh^3/[12(1-\mu^2)]$ 为板的抗弯刚度; μ 为泊松比, $\nabla^2 = \frac{\partial^2}{\partial x^2} + \frac{\partial^2}{\partial y^2}$ 为 Laplace 算子。

该模型中考虑单层板的面内位移 u 和 v , 以及面外位移 w , 其动能可表示为:

$$T = \frac{1}{2} \rho h \iint \sum_{i=1}^N (\dot{u}_i^2 + \dot{v}_i^2 + \dot{w}_i^2) dx dy \quad (5)$$

式中, ρ 为板的密度; \dot{u} , \dot{v} 和 \dot{w} 分别表示对时间的一阶导数。

基于 Hamilton 原理, 最终的变分形式为:

$$\delta \int_{t_1}^{t_2} (U - T) dt = 0 \quad (6)$$

四边固支边界条件下, 边界处位移和转角固定, 其边界条件为:

$$w = 0, \frac{\partial w}{\partial x} = 0, \frac{\partial w}{\partial y} = 0 \quad (7a)$$

$$u_i = 0, \frac{\partial u_i}{\partial x} = 0, v_i = 0, \frac{\partial v_i}{\partial y} = 0 \quad (7b)$$

2 考虑层间剪切多层板模型的离散方程

任意层的位移函数可表示为:

$$u_i(x) = \Phi(x) q_i^u(x) \quad (8a)$$

$$v_i(x) = \Phi(x) q_i^v(x) \quad (8b)$$

$$w(x) = \Phi(x) q^w(x) \quad (8c)$$

式中, $x = [x, y]$;

$$q_i^u(x) = [u_i(x_1) \quad u_i(x_2) \quad \cdots \quad u_i(x_n)];$$

$$q_i^v(x) = [v_i(x_1) \quad v_i(x_2) \quad \cdots \quad v_i(x_n)];$$

$$q^w(x) = [w(x_1) \quad w(x_2) \quad \cdots \quad w(x_n)], n \text{ 为节点数。}$$

$\Phi(x)$ 为基于移动 Kriging 插值的形函数, 表示为:

$$\Phi(x) = p^T(x) A + r^T(x) B \quad (9a)$$

其中,

$$A = (P^T R^{-1} P)^{-1} P^T R^{-1} \quad (9b)$$

$$B = R^{-1} (I - PA) \quad (9c)$$

式(9b)中 R 可表示为:

$$R = \begin{bmatrix} 1 & \gamma(x_1, x_2) & \cdots & \gamma(x_1, x_n) \\ \gamma(x_2, x_1) & 1 & \cdots & \gamma(x_2, x_n) \\ \cdots & \cdots & \cdots & \cdots \\ \gamma(x_n, x_1) & \cdots & \gamma(x_n, x_{n-1}) & 1 \end{bmatrix} \quad (10a)$$

$$\gamma(x, x_i) = \gamma(\psi) = 2 \left(1 - e^{-\theta \left(\frac{\psi}{a_0} \right)^2} \right), \quad \psi \leq a_0 \quad (10b)$$

式中, $\psi = \|x - x_i\|$ 为点 x 与 x_i 之间的距离; $\theta = 1$ 为相关参数; $a_0 = 3\|x - x_i\|$ 为影响域。

式(9b)中 P 可表示为:

$$P = \begin{bmatrix} p_1(x_1) & \cdots & p_m(x_1) \\ \vdots & \vdots & \vdots \\ p_1(x_n) & \cdots & p_m(x_n) \end{bmatrix} \quad (11a)$$

$$p^T(x) = [1 \quad x \quad y \quad x^2 \quad xy \quad y^2] \quad (11b)$$

式中, m 为多项式基的项数。

任意层的层内拉伸刚度矩阵可表示为:

$$K_{T_i} = \iint B_{T_i}^T D_T B_{T_i} dx dy \quad (12)$$

$$\text{式中, } B_{T_i}^T = \begin{bmatrix} \Phi_{,x} & & \\ & \Phi_{,y} & \\ \Phi_{,y} & \Phi_{,x} & \end{bmatrix}$$

层间剪切包括三部分,第一部分为相邻层之间滑动产生的剪切变形,其刚度矩阵可表示为:

$$K_{S_i}^1 = \iint B_{S_i}^T D_s B_{S_i} dx dy \quad (13)$$

$$\text{式中 } B_{S_i}^T = \begin{bmatrix} \Phi/h_1 & & \\ & \Phi/h_1 & \\ & & \Phi_{,xy} \end{bmatrix}, D_s = \begin{bmatrix} G_x & \\ & G_y \end{bmatrix}$$

第二部分为面内弯曲产生的剪切变形,其刚度矩阵为:

$$K_s^2 = \iint C^T D_s C dx dy \quad (14)$$

$$\text{式中, } C^T = \begin{bmatrix} \Phi_{,x} \\ \Phi_{,y} \end{bmatrix}$$

第三部分为上述两者之间产生的耦合矩阵:

$$K_{S_i}^3 = \iint B_{S_i}^T D_s C_i dx dy \quad (15a)$$

$$K_{\text{total}} = \begin{bmatrix} K_{T1} + K_{S1}^1 & -K_{S1}^1 & & & & -K_{S1}^4 \\ -K_{S2}^1 & K_{T2} + 2K_{S2}^1 & -K_{S2}^1 & & & \\ & & \dots & & & \\ & & & -K_{S(N-1)}^1 & K_{T(N-1)} + 2K_{S(N-1)}^1 & -K_{S(N-1)}^1 \\ & & & -K_{SN}^1 & K_{TN} + K_{SN}^1 & K_{SN}^4 \\ -K_{SN}^3 & & & & K_{SN}^3 & NK_D + (N-1)K_S^2 \end{bmatrix} \quad (19)$$

总的质量矩阵为:

$$M_{\text{total}} = \begin{bmatrix} M_1^1 & & & & & \\ & M_2^1 & & & & \\ & & \dots & & & \\ & & & M_{N-1}^1 & & \\ & & & & M_N^1 & \\ & & & & & NM^2 \end{bmatrix} \quad (20)$$

总的位移矩阵为:

$$q_{\text{total}}^T = [q_1 \quad q_2 \quad \dots \quad q_{N-1} \quad q_N \quad q^w] \quad (21)$$

式中, $q_i^T = [q_i^u \quad q_i^v]$, $i=1,2,\dots,N$ 。

3 考虑层间剪切的单层板模型振动

本节的纳米板以二硫化钼为研究对象,其物理参数见表1。为验证所建立模型的准确性,将分子动力学模拟的结果与所建立多层板模型的结果进行对比。本节分子动力学采用Lammps程序包进行模拟,通过第二代Brenner经验势来描述二硫化钼原子间的相互作用。

表1 多层板物理参数^[25]

$D/(\text{N}\cdot\text{m})$	μ	$\rho/(\text{kg}\cdot\text{m}^{-3})$	h/nm
2.4369×10^{-18}	0.31	9680.2	0.323

$$K_{S_i}^4 = \iint C_i^T D_s B_{S_i} dx dy \quad (15b)$$

任意层弯曲能的刚度矩阵为:

$$K_D = \iint B_D^T D_D B_D dx dy \quad (16)$$

其中,

$$B_D^T = \begin{bmatrix} 0 & 0 & \Phi_{,xx} \\ 0 & 0 & \Phi_{,yy} \\ 0 & 0 & 2\Phi_{,xy} \end{bmatrix}, D_D = D \begin{bmatrix} 1 & \mu \\ \mu & 1 \\ & & 1 - \mu/2 \end{bmatrix}$$

为方便最终刚度矩阵的组装,将任意层的质量矩阵分为面内质量矩阵和面外质量矩阵两部分:

$$M_i^1 = \rho h \iint N_i^T N_i dx dy \quad (17a)$$

$$M_i^2 = \rho h \iint \Phi^T \Phi dx dy \quad (17b)$$

$$\text{式中, } N_i^T = \begin{bmatrix} \Phi \\ \Phi \end{bmatrix}$$

最终离散方程组可表示为:

$$(K_{\text{total}} - \omega^2 M_{\text{total}}) q_{\text{total}} = 0 \quad (18)$$

其中,总的刚度矩阵为:

对于多层二硫化钼结构可近似为各向同性材料,其 xz 和 yz 面内的剪切模量分别为 $G_x=G_y=7.54$ GPa,层间厚度为 $h_1=0.64$ nm^[24]。模型的长为 $a=6$ nm,宽为 $b=8$ nm,边界条件为四边固支。

图2分别为采用分子动力学(MD),多层纳米板模型(MPSM)以及多层纳米板等效单层Kirchhoff板模型(KPM)和Mindlin板模型(MPM)计算得到的1~6层二硫化钼的前4阶振动频率 ω 。

图3为分子动力学和多层纳米板模型的前4阶振型。可以看出分子动力学的振动频率与振型和本文所建立的多层纳米板模型的结果吻合得非常好,而等效的单层Kirchhoff板模型和Mindlin板模型的振动频率都高于分子动力学结果。这表明多层二维结构层间剪切和滑移导致经典板理论不再适用。主要归因于二维结构之间的层间剪切和滑移与层内变形(拉伸和弯曲)存在竞争,并影响其整体动力学行为。

图4为不同长度多层纳米板的振动频率,可以看出,随着长度的增加,多层纳米板的振动频率逐渐减小。随着层数的增加,同一长度对应的同一阶振动频率逐渐增加,与此同时振动频率增加的绝对值逐渐减小。该结论与非局部硬化模型的结论是一致的,因为随着长度的增加,无量纲非局部效应因子减小,此时振动频率也随之减小,即频率随着非局部因子的增大而提高^[43-44]。

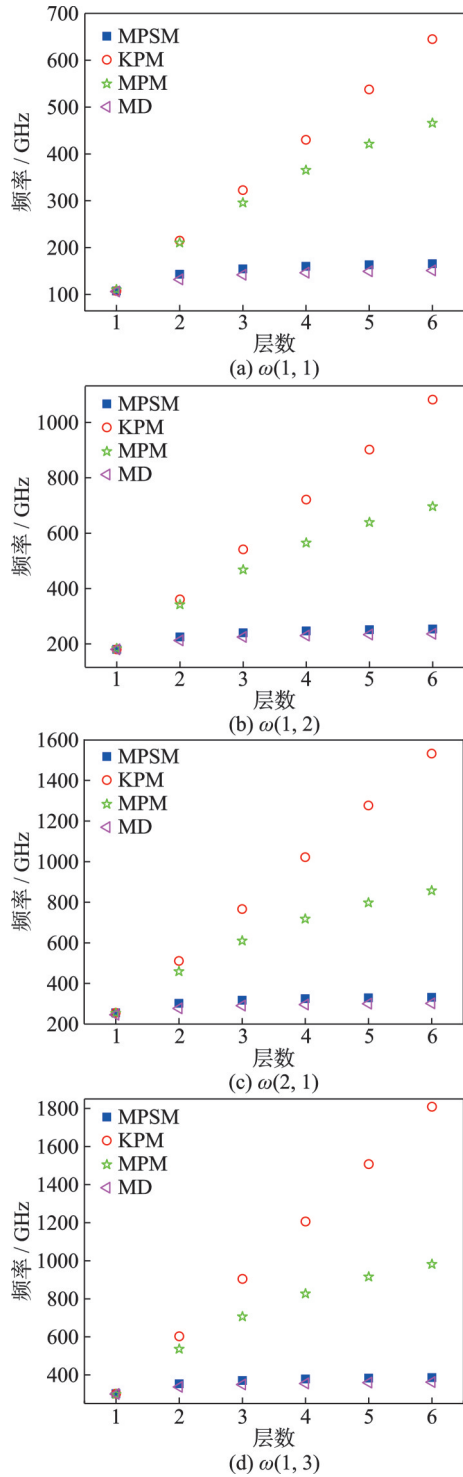


图 2 不同层数二硫化钼的频率
Fig. 2 Frequencies of MoS₂ for different layers

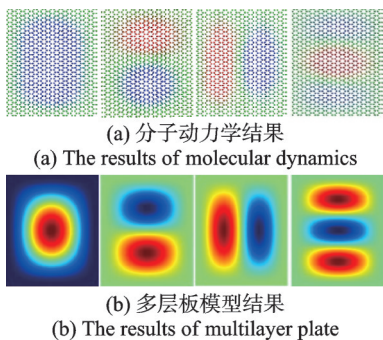


图 3 多层二硫化钼前 4 阶振型图
Fig. 3 First four order mode shapes of multilayer MoS₂

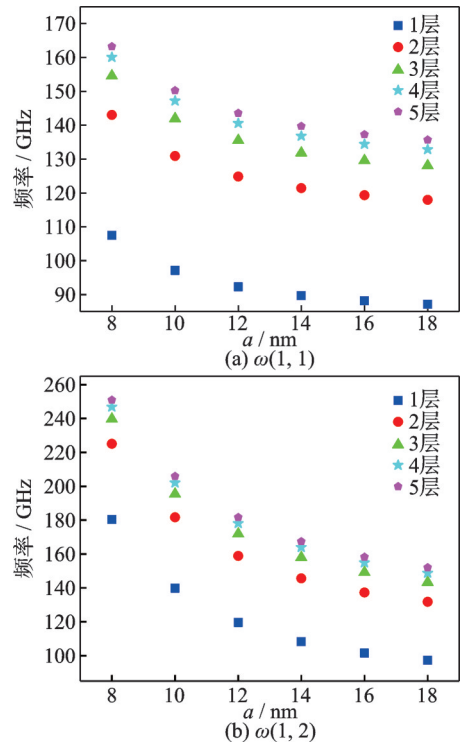


图 4 不同长度多层纳米板的振动频率 ($b=6\text{ nm}$)
Fig. 4 Frequencies of multilayer plates with different lengths ($b=6\text{ nm}$)

图 5 给出了不同层间剪切模量对振动频率的影响,图中横坐标 φ_1 代表剪切模量增加的倍数。结果表明,随着剪切模量的增加,频率逐渐增大。

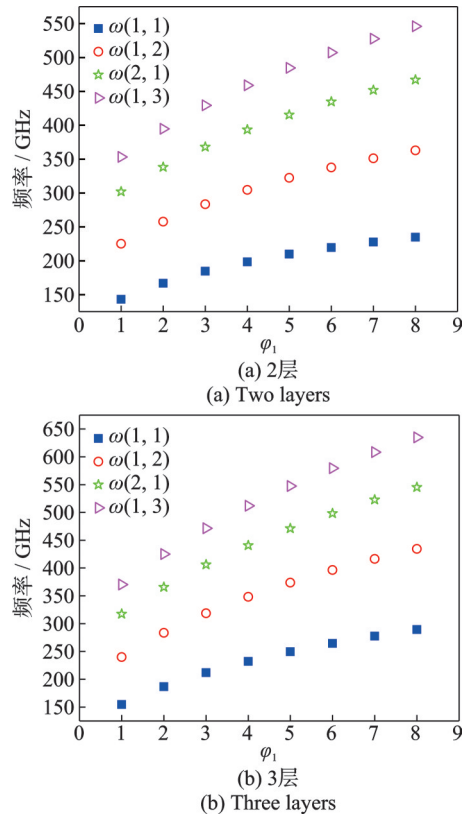


图 5 层间剪切模量与多层板振动频率的关系
Fig. 5 The relationship between interlayer shear modulus and frequencies of multilayer plates

图 6 为层内拉伸刚度与频率的关系,图中横坐标 φ_2 代表层内拉伸刚度增加的倍数。可以看出随着层内拉伸刚度的增加,频率几乎不发生改变。

图 7 为单层板弯曲刚度与频率的关系,图中横

坐标 φ_3 代表层内弯曲刚度增加的倍数。可以看出随着单层弯曲刚度的增加,频率逐渐增大。综上,层间剪切模量和单层弯曲刚度对横向振动频率的影响较大,而层内拉伸刚度的增加对横向振动频率几乎没有影响。

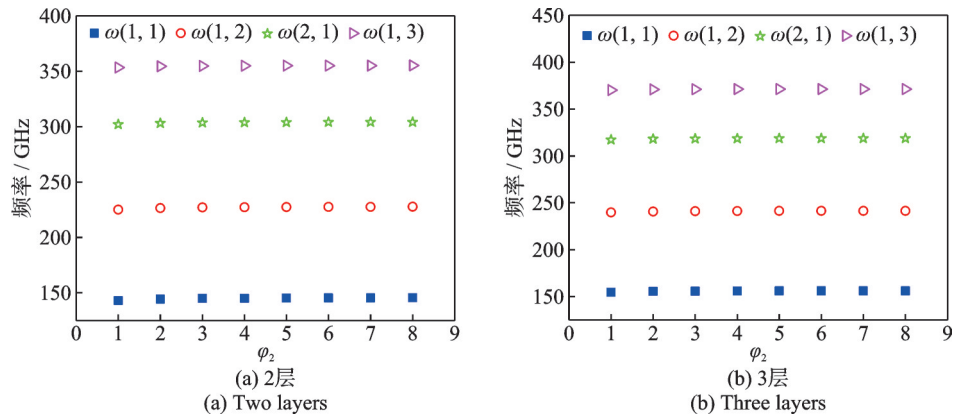


图 6 层内拉伸刚度与多层板振动频率的关系

Fig. 6 The relationship between intralayer tensile stiffness and frequencies of multilayer plates

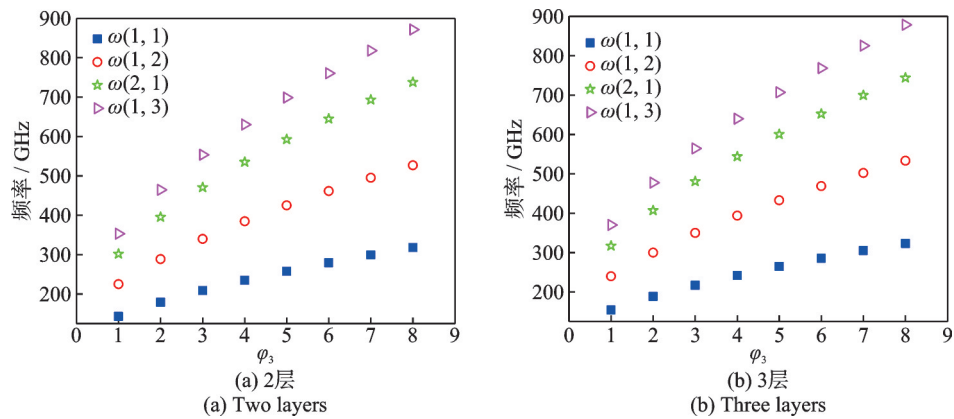


图 7 弯曲刚度与多层板振动频率的关系

Fig. 7 The relationship between bending stiffness and frequencies of multilayer plates

4 结 论

本文首先建立了考虑层内拉伸、层间剪切和单层弯曲的多层纳米板动力学模型。以二硫化钼为研究对象,并基于移动Kriging插值的无网格法计算了多层纳米板模型的振动频率,以及多层二硫化钼等效为单层Kirchhoff板和Mindlin板的振动频率。通过与分子动力学模拟的结果比较表明,建立的多层纳米板模型能够很好地预测多层二硫化钼的振动行为。这也说明多层二维结构层间剪切和滑移导致其违背了经典板理论的预测,主要归因于,二维结构之间的层间剪切影响了其整体动力学行为。随后分析了不同层数和尺寸对振动频率的影响,并通过改变层内拉伸刚度、层间剪切模量和单层弯曲刚度的大小来研究三者对振动频率的影响。研究表明,改变

层内拉伸刚度几乎不改变多层纳米板的振动频率,而改变层间剪切模量和单层弯曲刚度对振动频率的影响较大。

参考文献:

- [1] ZHAO Y D, QIAO J S, YU P, et al. Extraordinarily strong interlayer interaction in 2D layered PtS_2 [J]. *Advanced Materials*, 2016, 28(12): 2399-2407.
- [2] ZHAN H, GUO D, XIE G X. Two-dimensional layered materials: from mechanical and coupling properties towards applications in electronics[J]. *Nanoscale*, 2019, 11(28): 13181-13212.
- [3] DAI Z H, LIU L Q, ZHANG Z. Strain engineering of 2D materials: issues and opportunities at the interface [J]. *Advanced Materials*, 2019, 31(45): 1805417.
- [4] CONLEY H, LAVRIK N V, PRASAI D, et al. Graphene bimetallic-like cantilevers: probing graphene/sub-

- strate interactions[J]. *Nano Letters*, 2011, 11(11): 4748-4752.
- [5] BERTOLAZZI S, BRIVIO J, KIS A. Stretching and breaking of ultrathin MoS₂[J]. *ACS Nano*, 2011, 5(12): 9703-9709.
- [6] KOENIG S P, BODDETI N G, DUNN M L, et al. Ultrastrong adhesion of graphene membranes[J]. *Nature Nanotechnology*, 2011, 6(9): 543-546.
- [7] WANG G R, DAI Z H, XIAO J K, et al. Bending of multilayer van der Waals materials[J]. *Physical Review Letters*, 2019, 123(11): 116101.
- [8] DENG Z, SMOLYANITSKY A, LI Q Y, et al. Adhesion-dependent negative friction coefficient on chemically modified graphite at the nanoscale[J]. *Nature Materials*, 2012, 11(12): 1032-1037.
- [9] FILLETER T, MCCHESENEY J L, BOSTWICK A, et al. Friction and dissipation in epitaxial graphene films[J]. *Physical Review Letters*, 2009, 102(8): 086102.
- [10] FALIN A, CAI Q, SANTOS E J G, et al. Mechanical properties of atomically thin boron nitride and the role of interlayer interactions[J]. *Nature Communications*, 2017, 8: 15815.
- [11] WEI X D, MENG Z X, RUIZ L, et al. Recoverable slippage mechanism in multilayer graphene leads to repeatable energy dissipation[J]. *ACS Nano*, 2016, 10(2): 1820-1828.
- [12] YAMASHITA K, WAKE N, ARAKI T, et al. Human lymphocyte antigen expression in hydatidiform mole: androgenesis following fertilization by a haploid sperm[J]. *American Journal of Obstetrics and Gynecology*, 1979, 135(5): 597-600.
- [13] BLAKSLEE O L, PROCTOR D G, SELDIN E J, et al. Elastic constants of compression-annealed pyrolytic graphite[J]. *Journal of Applied Physics*, 1970, 41(8): 3373-3382.
- [14] LIU Z, ZHANG S M, YANG J R, et al. Interlayer shear strength of single crystalline graphite[J]. *Acta Mechanica Sinica*, 2012, 28(4): 978-982.
- [15] ZHENG Q S, JIANG B, LIU S P, et al. Self-retracting motion of graphite microflakes[J]. *Physical Review Letters*, 2008, 100(6): 067205.
- [16] LIU Z, YANG J R, GREY F, et al. Observation of microscale superlubricity in graphite[J]. *Physical Review Letters*, 2012, 108(20): 205503.
- [17] BOSAK A, KRISCH M, MOHR M, et al. Elasticity of single-crystalline graphite: inelastic X-ray scattering study[J]. *Physical Review B*, 2007, 75(15): 153408.
- [18] SHEN Y K, WU H G. Interlayer shear effect on multilayer graphene subjected to bending[J]. *Applied Physics Letters*, 2012, 100(10): 101909.
- [19] ZHANG K, TADMOR E B. Energy and moiré patterns in 2D bilayers in translation and rotation: a study using an efficient discrete-continuum interlayer potential[J]. *Extreme Mechanics Letters*, 2017, 14: 16-22.
- [20] LEBEDEVA I V, KNIZHNIK A A, POPOV A M, et al. Interlayer interaction and relative vibrations of bilayer graphene[J]. *Physical Chemistry Chemical Physics*, 2011, 13(13): 5687-5695.
- [21] LIU D Y, CHEN W Q, ZHANG C. Improved beam theory for multilayer graphene nanoribbons with interlayer shear effect[J]. *Physics Letters A*, 2013, 377(18): 1297-1300.
- [22] LIU Y L, XU Z P, ZHENG Q S. The interlayer shear effect on graphene multilayer resonators[J]. *Journal of the Mechanics and Physics of Solids*, 2011, 59(8): 1613-1622.
- [23] HUANG Z Z, HE Z Z, ZHU Y B, et al. A general theory for the bending of multilayer van der Waals materials[J]. *Journal of the Mechanics and Physics of Solids*, 2023, 171: 105144.
- [24] LIU R M, WANG L F. Nonlinear forced vibration of bilayer van der Waals materials drum resonator[J]. *Journal of Applied Physics*, 2020, 128(14): 145105.
- [25] ZHANG J C, LIU R M, WANG L F. Negative interlayer shear effect on a double-layered van der Waals material resonator[J]. *Physical Review B*, 2021, 104(8): 085437.
- [26] ZHANG J C, HOU D C, LIU R M, et al. Effect of stacking order on the vibration properties of bilayer black phosphorus[J]. *Proceedings of the Royal Society A-Mathematical Physical and Engineering Sciences*, 2022, 478(2263): 20220294.
- [27] LIU R M, HE J Y, ZHANG J C, et al. Moiré tuning of the dynamic behavior of a twisted bilayer van der Waals material resonator[J]. *Journal of Applied Mechanics*, 2022, 89(12): 121001.
- [28] CHEN Y H, ALIABADI M H. Meshfree-based micro-mechanical modelling of twill woven composites[J]. *Composites Part B:Engineering*, 2020, 197: 108190.
- [29] DEHGHAN M, NARIMANI N. The element-free Galerkin method based on moving least squares and moving Kriging approximations for solving two-dimensional tumor-induced angiogenesis model[J]. *Engineering with Computers*, 2020, 36(4): 1517-1537.
- [30] SUN Y Z, LIEW K M. The buckling of single-walled carbon nanotubes upon bending: the higher order gradient continuum and mesh-free method[J]. *Computer Methods in Applied Mechanics and Engineering*, 2008, 197(33-40): 3001-3013.
- [31] SUN Y Z, LIEW K M. Application of the higher-order Cauchy-Born rule in mesh-free continuum and multi-scale simulation of carbon nanotubes[J]. *International*

- Journal for Numerical Methods in Engineering, 2008, 75(10): 1238-1258.
- [32] YAN J W, LIEW K M, HE L H. Analysis of single-walled carbon nanotubes using the moving Kriging interpolation[J]. Computer Methods in Applied Mechanics and Engineering, 2012, 229: 56-67.
- [33] YAN J W, LIEW K M, HE L H. A mesh-free computational framework for predicting buckling behaviors of single-walled carbon nanocones under axial compression based on the moving Kriging interpolation[J]. Computer Methods in Applied Mechanics and Engineering, 2012, 247: 103-112.
- [34] YAN J W, LAI S K. Superelasticity and wrinkles controlled by twisting circular graphene[J]. Computer Methods in Applied Mechanics and Engineering, 2018, 338: 634-656.
- [35] ROQUE C M C, FERREIRA A J M, REDDY J N. Analysis of Mindlin micro plates with a modified couple stress theory and a meshless method[J]. Applied Mathematical Modelling, 2013, 37(7): 4626-4633.
- [36] THAI C H, HUNG P T, NGUYEN-XUAN H, et al. A size-dependent meshfree approach for magneto-electro-elastic functionally graded nanoplates based on nonlocal strain gradient theory[J]. Engineering Structures, 2023, 292: 116521.
- [37] THAI C H, FERREIRA A J M, NGUYEN-XUAN H, et al. A nonlocal strain gradient analysis of laminated composites and sandwich nanoplates using meshfree approach[J]. Engineering with Computers, 2023, 39: 5-21.
- [38] WANG B B, LU C S, FAN C Y, et al. A stable and efficient meshfree Galerkin method with consistent integration schemes for strain gradient thin beams and plates [J]. Thin-Walled Structures, 2020, 153: 106791.
- [39] WANG B B, LU C S, FAN C Y, et al. A meshfree method with gradient smoothing for free vibration and buckling analysis of a strain gradient thin plate[J]. Engineering Analysis with Boundary Elements, 2021, 132: 159-167.
- [40] ALSHENAWY R, SAFAEI B, SAHMANI S, et al. Buckling mode transition in nonlinear strain gradient-based stability behavior of axial-thermal-electrical loaded FG piezoelectric cylindrical panels at microscale[J]. Engineering Analysis with Boundary Elements, 2022, 141: 36-64.
- [41] YANG Z C, SAFAEI B, SAHMANI S, et al. A couple-stress-based moving Kriging meshfree shell model for axial postbuckling analysis of random checkerboard composite cylindrical microshells[J]. Thin-Walled Structures, 2022, 170: 108631.
- [42] LIU H W, SAFAEI B, SAHMANI S. Combined axial and lateral stability behavior of random checkerboard reinforced cylindrical microshells via a couple stress-based moving Kriging meshfree model[J]. Archives of Civil and Mechanical Engineering, 2021, 22(1): 15.
- [43] LIM C W. On the truth of nanoscale for nanobeams based on nonlocal elastic stress field theory: equilibrium, governing equation and static deflection[J]. Applied Mathematics and Mechanics, 2010, 31(1): 37-54.
- [44] LI C. A nonlocal analytical approach for torsion of cylindrical nanostructures and the existence of higher-order stress and geometric boundaries[J]. Composite Structures, 2014, 118: 607-621.

第一作者: 侯东昌(1991—),男,博士研究生。

E-mail: houdongchang@nuaa.edu.cn

通信作者: 王立峰(1977—),男,博士,教授。

E-mail: walfe@nuaa.edu.cn